

Investigating Charge Dispersion in GADGET II

Tyler Wheeler

August 2020

1 Introduction

1.1 Astrophysical Motivation

When a neutron star is orbited by a low-mass ($\lesssim 1.5M_{\odot}$) population II star it will accrete hydrogen-rich material from this binary companion. The temperatures and densities on the surface of the neutron star are such that the accreted hydrogen is continuously fused into helium via the hot-CNO cycle. Eventually the helium is ignited and a thermonuclear runaway proceeds. This can lead to the synthesis of proton-rich nuclides up to mass number 100, and extremely powerful x-ray bursts [5]. We measure these x-ray bursts using space based telescopes, and these data form what are called "light curves". The shape of

REACTIONS THAT IMPACT THE BURST LIGHT CURVE
IN THE MULTI ZONE X-RAY BURST MODEL.

Rank	Reaction
1	$^{15}\text{O}(\alpha,\gamma)^{19}\text{Ne}$
2	$^{56}\text{Ni}(\alpha,p)^{59}\text{Cu}$
3	$^{59}\text{Cu}(p,\gamma)^{60}\text{Zn}$
4	$^{61}\text{Ga}(p,\gamma)^{62}\text{Ge}$
5	$^{22}\text{Mg}(\alpha,p)^{25}\text{Al}$
6	$^{14}\text{O}(\alpha,p)^{17}\text{F}$
7	$^{23}\text{Al}(p,\gamma)^{24}\text{Si}$
8	$^{18}\text{Ne}(\alpha,p)^{21}\text{Na}$
9	$^{63}\text{Ga}(p,\gamma)^{64}\text{Ge}$
10	$^{19}\text{F}(p,\alpha)^{16}\text{O}$
11	$^{12}\text{C}(\alpha,\gamma)^{16}\text{O}$
12	$^{26}\text{Si}(\alpha,p)^{29}\text{P}$
13	$^{17}\text{F}(\alpha,p)^{20}\text{Ne}$
14	$^{24}\text{Mg}(\alpha,\gamma)^{28}\text{Si}$
15	$^{57}\text{Cu}(p,\gamma)^{58}\text{Zn}$
16	$^{60}\text{Zn}(\alpha,p)^{63}\text{Ga}$
17	$^{17}\text{F}(p,\gamma)^{18}\text{Ne}$
18	$^{40}\text{Sc}(p,\gamma)^{41}\text{Ti}$
19	$^{48}\text{Cr}(p,\gamma)^{49}\text{Mn}$

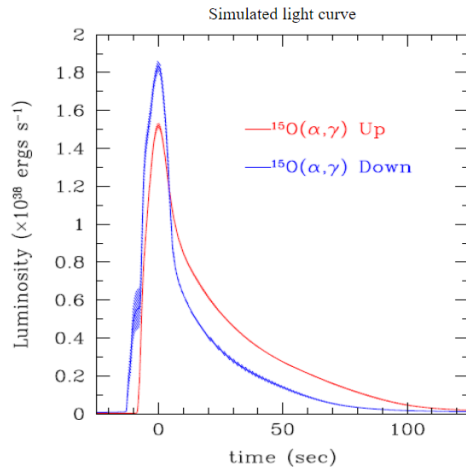


Figure 1: Left: Table ranking the sensitivity of light curve models to each of the relevant nuclear reaction rates. Right: Simulated plot of light curve intensity as a function of time using both the upper and lower limit for the $^{15}\text{O}(\alpha, \gamma)^{19}\text{Ne}$ reaction rate [1].

the light curve can in principle tell you interesting things about the neutron

star itself, but there are a lot of nuclear physics uncertainties associated with the shape of the light curve. Modeling x-ray burst light curves has shown that the $^{15}\text{O}(\alpha, \gamma)^{19}\text{Ne}$ reaction is the most important reaction underlying the shape of the light curve (Fig. 1). As such, we have proposed an experiment to measure this reaction rate at the Facility for Rare Isotope Beams at Michigan State University.

1.2 Constraining the Reaction

Ideally, we would measure the $^{15}\text{O}(\alpha, \gamma)^{19}\text{Ne}$ reaction directly, but given that ^{15}O is radioactive this is not currently a possibility. Thankfully, the reaction has only one resonance that determines the rate of the reaction; the 4.03 MeV resonance in ^{19}Ne . Previous measurements taken by our group have shown that this state is populated in the decay sequence of ^{20}Mg [9]. Figure 2 illustrates

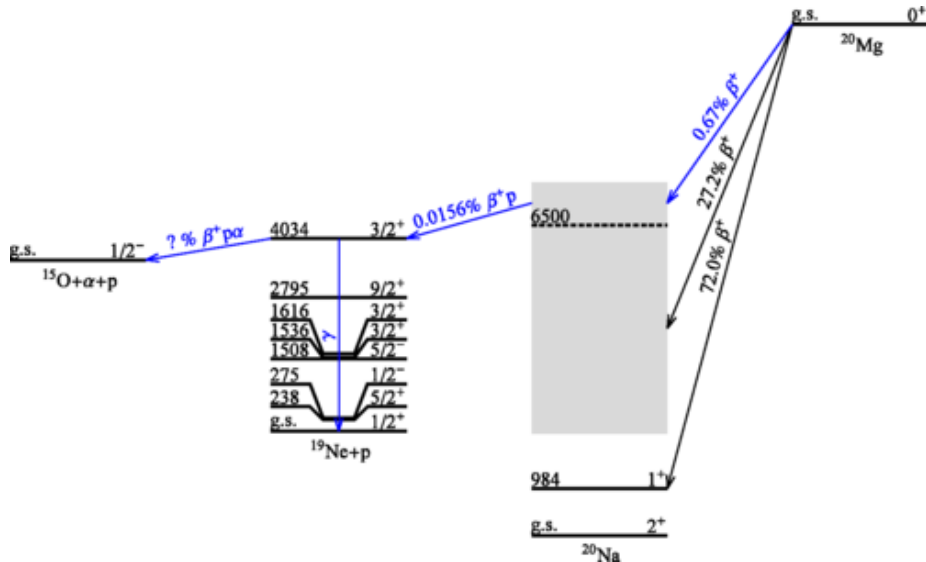


Figure 2: Decay sequence of ^{20}Mg showing the β -delayed proton emission that leads to the population of the 4.03 MeV state in ^{19}Ne .

that a $^{20}\text{Mg}(\beta p \alpha)^{15}\text{O}$ event through the key $^{15}\text{O}(\alpha, \gamma)^{19}\text{Ne}$ resonance yields a characteristic signature, namely, the near simultaneous emission of a proton and alpha particle. Thus, to measure this reaction we need a detector capable of detecting both protons and alphas, and distinguishing between them.

2 GADGET II

2.1 Upgrading GADGET to a TPC

GADGET stands for Gaseous Detector with Germanium Tagging, and it was built to detect individual protons emitted after beta decays. However, GADGET is ill-equipped for detecting multiple particle emissions and distinguishing between them. But as we've learned from section 1.2, the characteristic signature of the state we're populating is the near simultaneous emission of a proton and alpha particle. To achieve the granularity necessary for the identification of this characteristic signature, we are transforming GADGET into a time projection chamber (TPC) called GADGET II, which will allow us to reconstruct 3D images of the events that take place in our detector. GADGET II can be

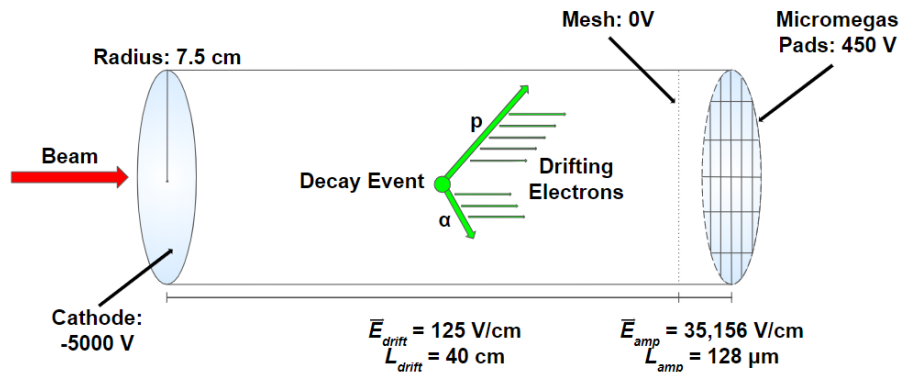


Figure 3: Rough schematic of the GADGET II TPC. Note that the electric field in the drift region, E_{drift} , and in the amplification region, E_{amp} , are both pointing toward the left side of the page causing the ionized electrons to drift toward the right.

thought of as having two distinct regions; a drift region, and proportional amplification region (Fig. 3). The electric field in the drift region is tuned such that the ionized electrons make their way to the mesh without liberating any additional charge. Conversely, the proportional amplification region is characterized by a strong electric field that generates a Townsend avalanche, effectively amplifying event signals. After traversing this short distance, the charge cluster will be collected on a resistive anode that will induce a charge on our Micromegas pads (the function of the resistive anode is discussed further in section 2.2). The Micromegas will contain over one thousand $2.2 \times 2.2 \text{ mm}$ pads, which will give us our needed spatial resolution to construct a 2D image of a decay event. The third dimension in our image reconstruction will come from the time-of-flight differences for the arriving electrons. Once 3D images of decay events are constructed we will use a machine learning algorithm, possibly a convolutional neural network, to identify the topology unique to our events of interest.

2.2 Distributed RC Network

A novel method for improving the spatial resolution of detectors analogous to ours, involves the utilization of charge dispersion with a thin resistive anode (see Fig. 4). In effect, the resistive anode uniformly disperses a deposited charge cluster allowing one to determine the charge centroid, and potentially yield sub-pad resolution [3]. The resistive anode lies atop a thin layer of Mylar, which is in turn affixed to the Micromegas readout plane with an insulating layer of glue. The Mylar and glue act as dielectrics in a two dimensional resistive-capacitive network. The resistance in this network is determined by the surface resistivity of the anode, and the capacitance is determined by the relative permittivity of the glue and Mylar, and the anode-readout plane separation. The equation for the capacitance per unit area for a parallel plate capacitor with two dielectrics can be written as:

$$C = \frac{2\epsilon_0}{d} \frac{k_1 k_2}{k_1 + k_2}, \quad (1)$$

where ϵ_0 is the permittivity of a vacuum, k_1 and k_2 are the relative permittivities of the dielectric materials, and d is the anode-readout plane separation. Note that although this distributed RC network can in principle provide us with improved spatial resolution, for our purposes we don't require sub-pad resolution. However, the resistive anode's inherent ability to protect our data acquisition system from electrical breakdown make it an invaluable addition to our detector. Just the same, an analysis must be done to home in on acceptable RC values for the network to ensure a spatial resolution on the order of our Micromegas pad size.

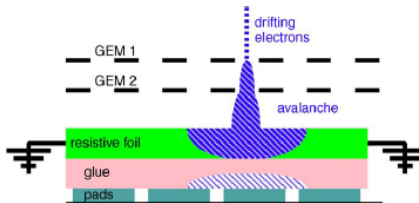


Figure 4: Schematic of the charge dispersion readout concept used in conjunction with two Gas Electron Multipliers [3].

3 Modeling Charge Dispersion on a Resistive Anode

3.1 Charge Density in an Ideal Case

The addition of a resistive anode to the readout plane of the detector works to create an RC network. We can begin modeling this network by utilizing the two dimensional Telegraph equation [2]:

$$\frac{\partial \rho}{\partial t} = h \left[\frac{\partial^2 \rho}{\partial r^2} + \frac{1}{r} \frac{\partial \rho}{\partial r} \right], \quad (2)$$

where ρ is the charge density, r is radial position, and $h = \frac{1}{RC}$ where R is the surface resistivity of the anode, and C is the capacitance given by Eq. 1. In the ideal case we take the resistive anode to have an infinite radius, and at $t = 0$ we assume there to be a point charge at the origin. Then the solution for the charge density is given by:

$$\rho(r, t) = \frac{1}{2th} \exp(-r^2/4th). \quad (3)$$

Using this equation we can plot the charge density as a function of radial position for various R and C values (see Fig. 5). For GADGET II the range of applicable surface resistivity values is between 2 and 10 $M\Omega$, and in Dixit's 2004 paper he uses an anode-readout plane separation of 100 μm , where 50 μm is the layer of glue and the other 50 μm is the layer of Mylar. Additionally, from Dixit's

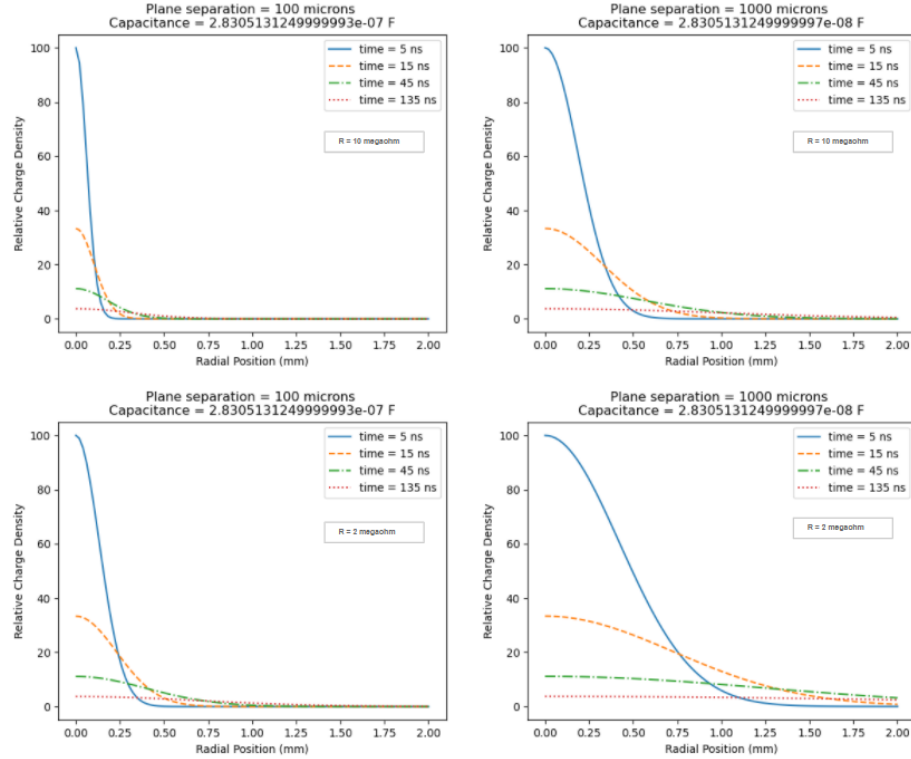


Figure 5: Evolution of the 2D charge density function on a resistive anode in an ideal case. Top Row: Resistivity = 10 $M\Omega$ per square. Bottom Row: Resistivity = 2 $M\Omega$ per square. Anode-readout plane separation is varied from 100 microns to 1000 microns.

example an assumption was made that as the separation increases the gap is always filled with half Mylar and half glue. However, given that the relative

permittivity of both the Mylar and glue are very close (3.1 and 3.3, respectively) any change in our results due small deviations from this assumption should be negligible. The plots in figure 5 show that the plane separation can be quite large, relative to Dixit's 100 μm example, and still retain most of the signal within a radius of 1 mm even at the lower bound surface resistivity of 2 M Ω .

3.2 Charge on an Individual Pad

Before we calculate the charge on an individual pad, Q_{pad} , let's briefly summarize the derivation for Q_{pad} provided in Dixit's 2006 paper [3]. We start by writing the Telegraph (Eq. 2) in terms of Cartesian coordinates:

$$\frac{\partial \rho}{\partial t} = h \left[\frac{\partial^2 \rho}{\partial x^2} + \frac{\partial^2 \rho}{\partial y^2} \right]. \quad (4)$$

Then, in order to ensure a closed form solution of Eq. 4 we assume a delta function point charge is collected at the origin at $t = 0$, to get:

$$\rho_{\delta}(x, y, t) = \left(\frac{1}{2\sqrt{\pi th}} \right)^2 \exp[-(x^2 + y^2)/4th]. \quad (5)$$

To account for the fact that the actual charge profile is described by a Gaussian, we convolve Eq. 5 with the Gaussian characterizing our charge cluster:

$$\rho(x, y, t) = \frac{Nq_e}{2\pi(2ht + w^2)} \exp[-(x^2 + y^2)/(2(2ht + w^2))], \quad (6)$$

where N represents the numbers of electrons, q_e is the electron charge, and w is the width of the Gaussian describing the charge cluster. From here we can integrate the charge density function over the area of a single pad to get the charge on a pad:

$$Q_{pad}(t) = \frac{Nq_e}{4} \left[\text{erf} \left(\frac{x_{high}}{\sqrt{2}\sigma_{xy}} \right) - \text{erf} \left(\frac{x_{low}}{\sqrt{2}\sigma_{xy}} \right) \right] \\ \times \left[\text{erf} \left(\frac{y_{high}}{\sqrt{2}\sigma_{xy}} \right) - \text{erf} \left(\frac{y_{low}}{\sqrt{2}\sigma_{xy}} \right) \right], \quad (7)$$

where x_{high} , x_{low} , y_{high} , and y_{low} represent the pad boundaries, and $\sigma_{xy} = \sqrt{2th + w^2}$. Now that we have derived an expression for Q_{pad} let's use it to calculate the charge on a pad for an event of interest; a 506 keV alpha particle in P10 gas (90% argon and 10% methane). We first need to determine the total amount of charge that will reach the resistive anode. The initial amount of ion pairs formed from the alpha particle ionization is given by:

$$n_0 = \frac{E_{alpha}}{W}, \quad (8)$$

where E_{alpha} is the energy of the alpha particle, and W , often referred to as the W-value, is the average energy lost by the incident particle per ion pair formed. The W-value is a function of gas type, radiation type and its corresponding energy, however, it's a fairly weak function of these parameters, meaning the W-value can often be treated as a constant for each gas [6]. Based on the literature we can assume that P10 has a W-value of $W \approx 26.73$ [8]. Thus, from Eq. 8 we find that approximately 18,930 ion pairs are initially formed. Then we need to determine the gas gain from the Townsend avalanche that occurs after the electrons pass through the mesh. An internal report from M. Roosa showed that the gas gain for P10 with an Electric field at 35.156 kV/cm is 221 [7]. Recall that gas gain can be written as:

$$Gain = \frac{N}{n_0}, \quad (9)$$

which tells us that the total number of electrons that reach the anode is about $N = 4,183,530$. Finally, to find the width of the Gaussian describing this charge cluster we need to determine the transverse diffusion of the electrons in the drift region of the detector. To accomplish this we can use the Magboltz program along with an API developed by Stephen Biagi which acts as a python wrapper to Magboltz. Simulating 10 million collisions gives us a transverse diffusion coefficient of $D_T = 0.9145 \times 10^4 \text{cm}^2/\text{s}$. Then we note that the standard deviation is given by:

$$\sigma = \sqrt{2D_T t_{drift}}, \quad (10)$$

where t_{drift} is the drift time. Our Magboltz simulation found the longitudinal velocity to be $55.28 \mu\text{m}/\text{ns}$, which gives us a drift time of $7.2 \mu\text{s}$ for the charge to drift the full 40 cm length of the drift region. However, our group has previously reported a drift time of $7.5 \mu\text{s}$, so we will use this value instead [4]. Thus, $\sigma = 0.3704 \text{cm}$. From here we calculate the Full Width Half Max (FWHM) as:

$$\text{FWHM} = 2\sqrt{2\ln(2)}\sigma = w. \quad (11)$$

This gives us $w = 8.722 \text{mm}$. At last, we have everything we need to use Eq. 7, and the resulting plots can be seen in Fig. 6 for both the shown example of a 506 keV alpha, as well as a 1.2 MeV proton.

4 Conclusion

The results from section 3.1 illustrate that the majority of our signal will stay within a 1 mm radial spread for a surface resistivity as low as $2 \text{M}\Omega$, and for a corresponding anode-readout plane separation as large as $1000 \mu\text{m}$. Furthermore, given that the GET data acquisition system that will be used with GADGET II has very little dead time, we don't require the charge on a pad to dissipate much before recording another signal. Thus, section 3.2 tells us that for a time window on the order of $10 \mu\text{s}$, and a plane separation of $100 \mu\text{m}$, we would want to use a surface resistivity value of $\approx 2 \text{M}\Omega$. However, in the case of

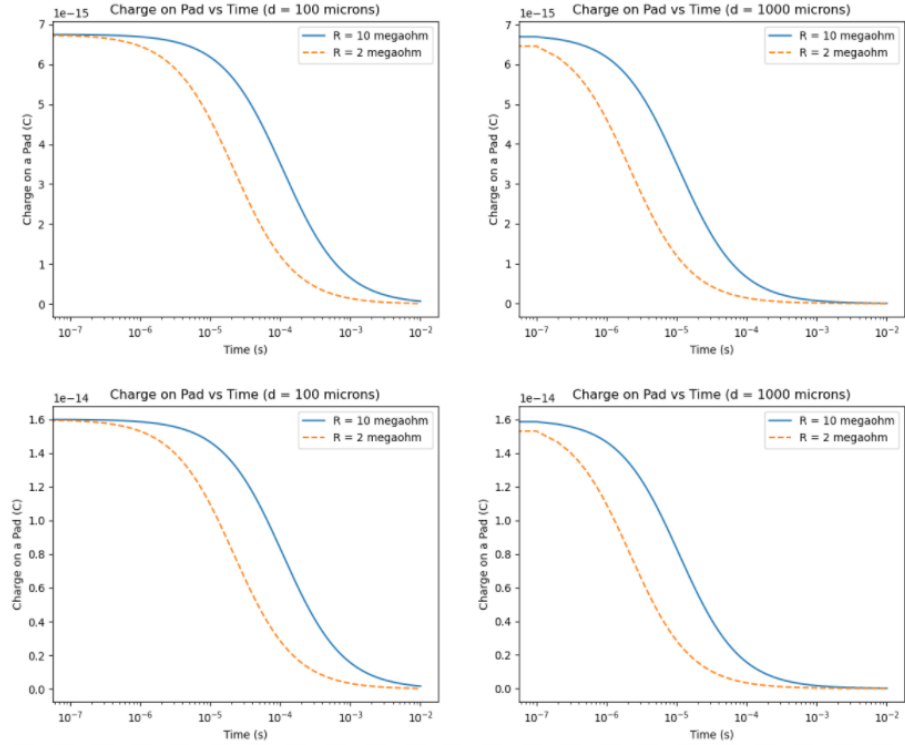


Figure 6: Charge on an individual 2.2×2.2 mm pad as a function of time. Charge is centered at the origin of the pad. The left plots use an anode-readout plane separation of 100 microns, and the right plots use a separation of 1000 microns. Top row simulates a 506 keV alpha, and bottom row simulates a 1.2 MeV proton, both in P10 gas.

a large plane separation ($\approx 1000\mu\text{m}$), then a surface resistivity value anywhere in between 2 and 10 $\text{M}\Omega$ should suffice for our purposes.

References

- [1] R.H. Cyburt. Dependence of x-ray burst models on nuclear reaction rates. *The Astrophysical Journal*, 830(2):55, 2016.
- [2] M.s. Dixit. Position sensing from charge dispersion in micro-pattern gas detectors with a resistive anode. *Nuclear Instruments and Methods in Physics Research Section A: Accelerators, Spectrometers, Detectors and Associated Equipment*, 518(3):721:727, 2004.
- [3] M.s. Dixit. Simulating the charge dispersion phenomena in micro pattern gas detectors with a resistive anode. *Nuclear Instruments and Methods in*

- Physics Research Section A: Accelerators, Spectrometers, Detectors and Associated Equipment*, 566(2):281:285, 2006.
- [4] M. Friedman. Gadget: a gaseous detector with germanium tagging. *Nuclear Instruments and Methods in Physics Research Section A: Accelerators, Spectrometers, Detectors and Associated Equipment*, 940, 2019.
 - [5] Christian Iliadis. *The Nuclear Physics of Stars*. Weinheim, 2007.
 - [6] Glenn F. Knoll. *Radiation detection and measurement*. John Wiley Sons, 2012.
 - [7] M. Roosa. *Simulating the Response of a New -Delayed Proton Detector*. 2018.
 - [8] H. Tawara. Energy dependences of w values for mev alpha particles in ar-xe, ar-n2, and ar-ch4 mixtures. *Nuclear Instruments and Methods in Physics Research Section B: Beam Interactions with Materials and Atoms*, 29(3), 1987.
 - [9] C. Wrede and B. Glassman. New portal to the $^{15}\text{o}(\alpha, \gamma)^{19}\text{ne}$ resonance triggering cno-cycle breakout. *Physical Review C*, 96(3), 2017.

A Magboltz API

A.1 Prerequisites

The Magboltz API, which acts as a python wrapper for the original Magboltz program written in FORTRAN, is used to calculate the transverse diffusion of a charge cluster. The API can be obtained by cloning the GitHub repository at: <https://github.com/UTA-REST/MAGBOLTZdev>. Note that the API uses python 2.7.12, so ensure that you have this version of python, as more recent versions are not compatible with this code.

A.2 Running the API

To run the program first use terminal to navigate to the directory where you extracted the Magboltz files. Then type "python2 Main.py" to run the program. A GUI will then open where all inputs can be entered (Fig. 7). Note that every text box must be filled in for the program to run, so you must put 0 for entries that are not applicable. The gas input values can be seen in Fig. 7, and a more comprehensive list can be found in the GitHub repository under "Database". After the program has finished running you can close the GUI and then you can use a text editor to open the output file (Output.txt).

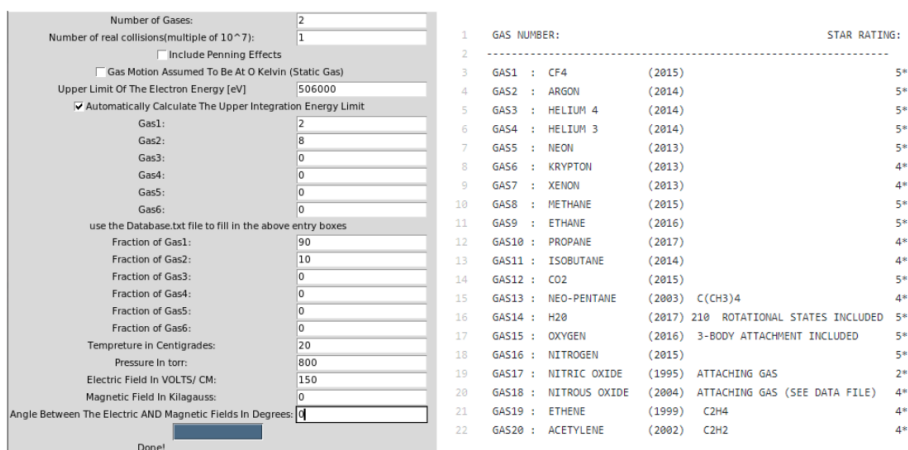


Figure 7: Left: GUI generated from Magboltz API with example inputs filled in. Right: Gas list database for gas inputs. The given inputs in the GUI show that the gas being simulated is P10.